Stress Dependence of Leaky Surface Wave on PMMA by Line-focus-beam Acoustic Microscope

by M. Obata, H. Shimada and T. Mihara

ABSTRACT—The authors discuss a line-focus-beam (LFB) acoustic microscope as a system for evaluating local stresses in polymeric materials. The goal of this paper is to reveal the stress-dependence of the velocity of the leaky surface skimming-compressional wave (LSSCW), which is excited by the LFB acoustic microscope and propagates on the boundary of the water/specimen surface.

M. Obata (SEM Member) is Professor, Department of Materials Processing, Faculty of Engineering, Tohoku University, Aramaki Aoba, Aobaku, Sendai, 980, Japan. H. Shimada (SEM Member) is President, Akita National College of Technology, Bunkyochou 1-1 Akita, 011, Japan. T. Mihara is Research Associate, Department of Materials Processing, Tohoku University.

Paper was presented at the 1988 SEM Spring Conference on Experimental Mechanics held in Portland, OR on June 5-10.

Original manuscript submitted: March 17, 1989. Final manuscript received: August 2, 1989.

Introduction

In order to employ polymeric materials in design with more efficiency and confidence, many technical problems remain unsolved. As one of these problems, the evaluation of stress in the local region is very important. Several nondestructive methods, for example an X-ray method, a magnetoelastic method[1,2] and an ultrasonic method[3] have been developed and mainly employed to evaluate residual stress in metallic materials. Among these methods, only an ultrasonic method is applicable to polymeric materials. It is impossible for these ordinary systems to analyze the detailed state of local stress because of the low space-resolution power of measurement. In order to overcome these disadvantages, the authors tried to employ an acoustic microscope as a system for the measurement of local stress in polymetric materials.

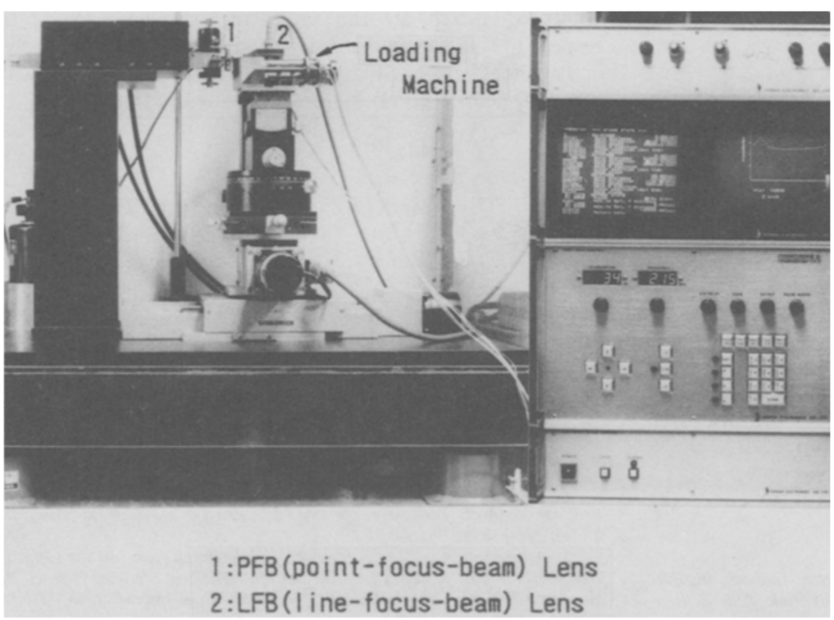

Fig. 1—Acoustic microscope with (1) PFB and (2) LFB lenses

A mechanical scanning acoustic microscope developed by Lemons and Quate[4] in 1973 has been improved and equipped to perform two main functions: (1) the acoustic imaging measurements in the scanning mode; (2) the quantitative measurement of both the velocity and the attenuation of leaky surface waves in the nonscanning mode. Recently the latter function has attracted attention and was advanced more powerfully as a system for microscopic material characterization by Chubachi[5] through the development of the line-focus-beam (LFB) lens. In this paper, the authors experimentally study the application of the LFB acoustic microscope as a system for evaluating local stress on the surface of polymeric materials. It is the goal of this paper to introduce the stress dependence of the velocity of a leaky surface wave experimentally which is excited by the LFB acoustic microscope. The discussion includes (1) formulation of acoustic anisotropy caused by uniaxial stress as a function of applied stress and propagation direction of leaky surface waves; (2) expansion of the results obtained in (1) to the state of plane stress by the principle of superposition; (3) verification of the resultant equation derived in eq (2) through a biaxial test and a bending test.

Experimental Procedure

Acoustic Microscope and Phase Velocity Measurement

The acoustic microscope used in this paper (Fig. 1) has two types of acoustic lens: (1) a point-focus-beam (PFB) lens; (2) a line-focus-beam (LFB) lens. The PFB lens focuses a plane wave transmitted from the ultrasonic transducer onto a point on a specimen surface and is mainly used for acoustic imaging measurements in the scanning mode. The LFB lens which was proposed by Chubachi[5] in 1981 formed a wedge-shape beam with a cylindrical wavefront. A wedge-shape beam linearly focuses along one axis on the specimen surface as shown in Fig. 2 and excites leaky surface waves in only one direction (in the case of Fig. 2, the x direction). Therefore, rotation of the specimen (or the LFB lens) around the beam axis allows us to detect acoustic anisotropies. The phase velocity of the leaky surface wave was determined through a $V(z)$ curve which was a variation of output signal from a piezoelectric transducer with the distance between an acoustic lens and a specimen surface. A typical $V(z)$ curve recorded in this study is shown in Fig. 3. As shown in Fig. 3, the output from a transducer varied periodically with changing the position of the specimen from a focal point ($z = 0$) toward a LFB lens (the negative z direction) along the z axis (beam axis) without scanning in x and y directions. These periodic dips are caused by interference of two components of the acoustic waves which were designated by #0 and #1 in Fig. 3, respectively. Experimental and theoretical works[5] on the $V(z)$ curves indicate that the periodicity of dips on the curve is closely related to the phase velocity of the leaky surface wave propagating along the boundary of the couplant/specimen surface (in the case of Fig. 3, #1). The phase velocity V_ℓ of the leaky surface wave can be calculated by eq (1).[5]

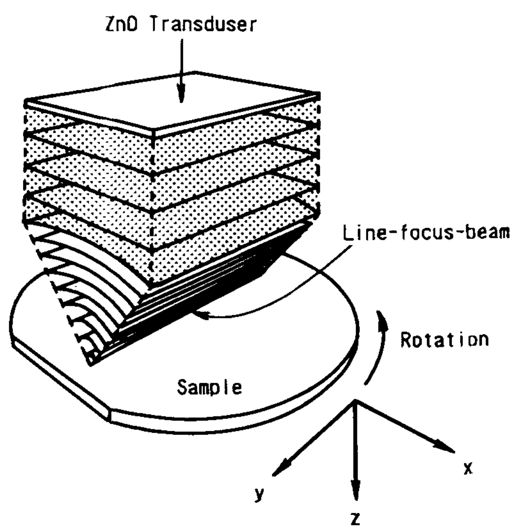

Fig. 2—Schematic illustration of focusing process by the LFB lens

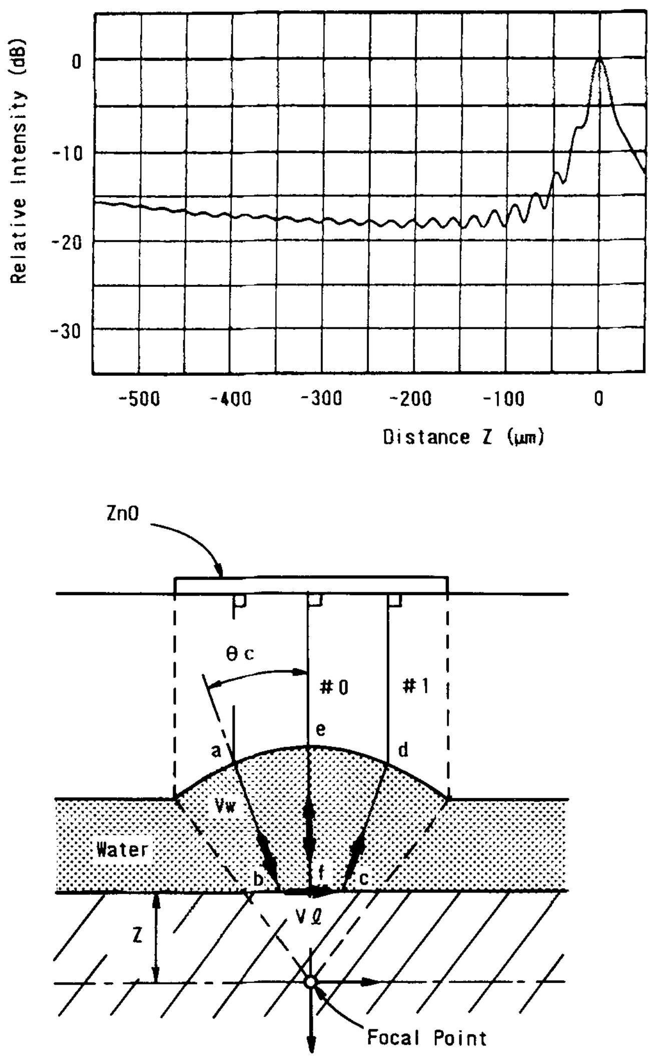

Fig. 3—Typical $V(z)$ curve of PMMA and cross-sectional geometry of LFB lens

$$V_\ell = V_w / \sqrt{\{1 - (1 - V_w/2f \cdot \Delta z)^2\}} \qquad (1)$$

where V_w = velocity in couplant, f = frequency. The dip interval Δz in the $V(z)$ curve was determined by applying a FFT analysis to a $V(z)$ curve and was input into eq (1). Repeats of $V(z)$ measurements at various directions (ϕ) around the z axis permit us to express V_ℓ as a function of direction.

Experimental Conditions

The experimental conditions are summarized in Table 1. The LFB lens used can measure acoustic velocity in an area smaller than 0.5 × 0.5 mm. Specimens were machined from an as-received PMMA plate whose surface was smooth enough to avoid velocity dispersion caused by surface roughness. Before loading, acoustic homogeneity and isotropy of each specimen was confirmed. The load was applied through a small loading machine (Fig. 4) with a load cell which was fixed on the top of a sample stage as shown in Fig. 1. When the load reached the level determined in advance, measurements of $V(z)$ curves were made in the desired directions around the z axis.

Confirmation of Excited Wave Mode

Chubachi confirmed and reported five kinds of leaky surface wave modes which are excited by the LFB acoustic microscope depending upon the boundary conditions. On the boundary of water (couplant)/semi-infinite polymeric specimen, only the excitation of the leaky surface skimming-compressional wave (LSSCW) can be expected to be possible, because usual polymeric materials have relatively smaller shear velocity than that of water. The FFT-analyzed spectrum (Fig. 5) of the $V(z)$ curve obtained from PMMA shown in Fig. 3 expectedly indicates the existence of only one mode of LSSCW having enough power to distinguish it from the noise level. The excitation of the other waves, for example the leaky Rayleigh wave,[6,7] could not be confirmed. This is the reason why we focus attention on the LSSCW wave mode in this paper.

TABLE 1—EXPERIMENTAL CONDITIONS

Acoustic Microscope	HONDA Electronic Co. Ltd.
Acoustic Lens	LFB (Line-focus-beam) Lens
Frequency	215 MHz
Couplant	Distilled Water
Velocity Measurement	$V(z)$ Curve Analysis
Specimen Material	PMMA (as received)
Wave Mode	LSSCW (Leaky Surface Skimming Compressional Wave)

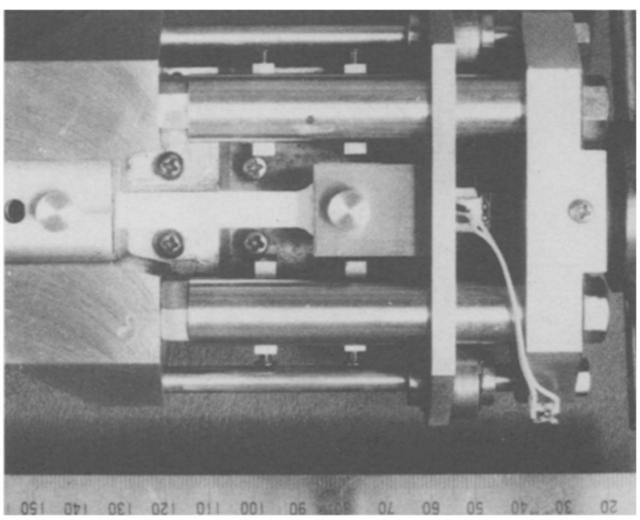

Fig. 4—Uniaxial loading machine which is fixed on the top of sample stage

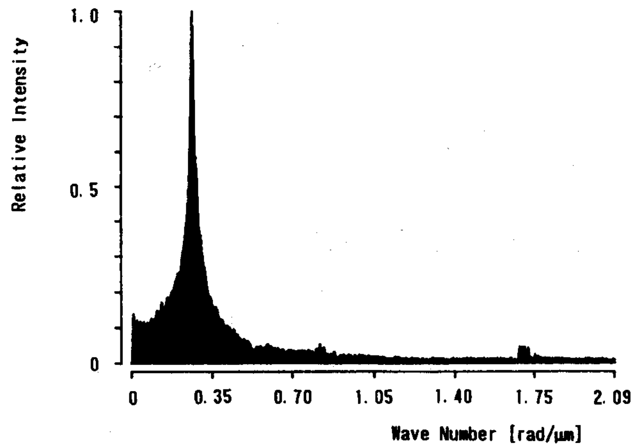

Fig. 5—Typical example of FFT-analyzed spectrum for the $V(z)$ curve obtained from PMMA

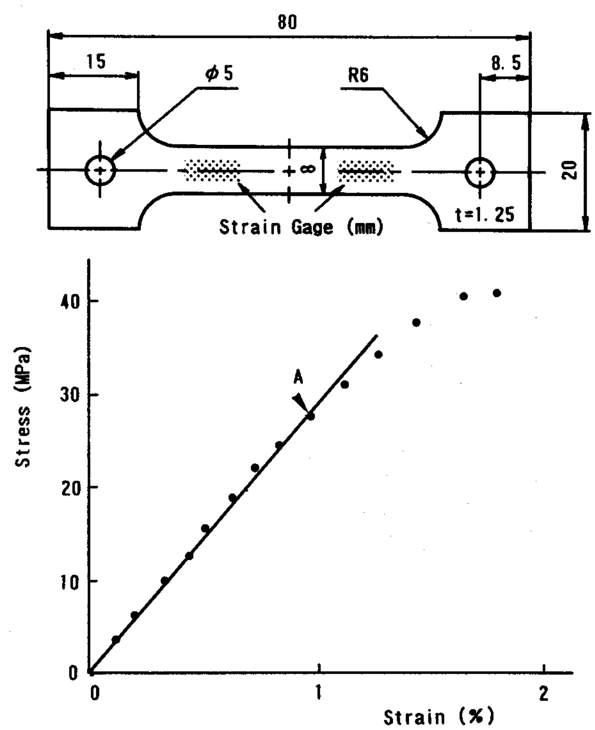

Fig. 6—Stress-strain curve of PMMA and dimensions of uniaxial specimen

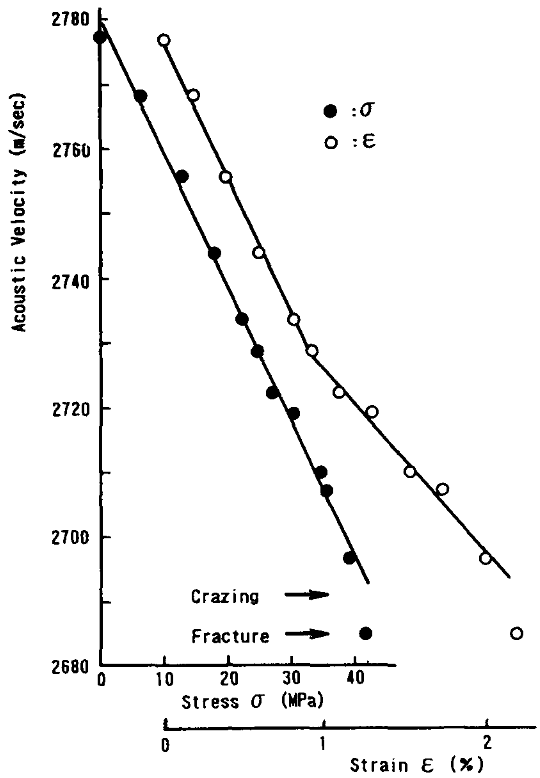

Fig. 7—Variation of acoustic velocity with stress and strain

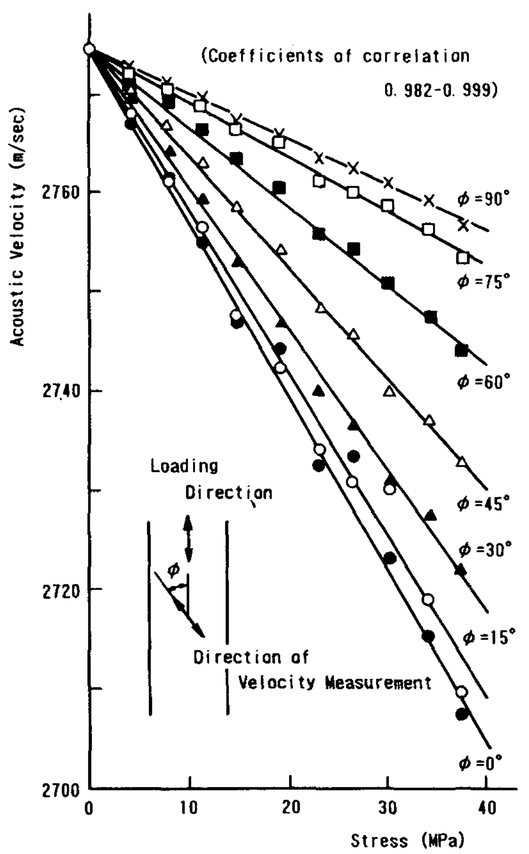

Fig. 8—Variation of acoustic velocity with uniaxial stress

Stress-dependence of LSSCW Velocity in the State of Uniaxial Stress

As the first step, uniaxial tests were made using the loading machine (Fig. 4) and a specimen (Fig. 6). Figure 7 shows the variations of LSSCW velocity V_ℓ in the loading direction with stress σ_y and strain ϵ_y. It was found from Fig. 7 that V_ℓ is proportional to σ_y in the region from σ_y = 0 to almost fracture. This result indicates that the relationship between LSSCW velocity and stress in the linear part of $\sigma_y - \epsilon_y$ curve can be applied beyond the point 'A' in Fig. 6 where σ_y varies nonlinearly with ϵ_y. Figure 8 shows variations of LSSCW velocity $V_\ell(\phi)$ in several directions of ϕ's (Fig. 8) with uniaxial stress σ_y. In each direction, $V_\ell(\phi)$ varied linearly with σ_y. However, each slope $\alpha(\phi)$ changed with ϕ as shown in Fig. 9. These variations shown in Fig. 8 and Fig. 9 can be formulated by eqs (2) and (3), respectively.

$$V_o - V_\ell(\phi) = \Delta V_\ell(\phi) = \alpha(\phi) \cdot \sigma_y \tag{2}$$

$$\alpha(\phi) = ½ \cdot \{[\alpha(0) + \alpha(90)] + [\alpha(0) - \alpha(90)] \cdot \cos 2\phi\} \tag{3}$$

where V_o = velocity at σ_y = 0; $\alpha(0)$, $\alpha(90)$ = values of α at ϕ = 0 and 90, respectively (experimental values of $\alpha(0)$ and $\alpha(90)$ were −1.917 and −0.644). Substituting eq (3) into eq (2), we can get the following eq (4) which shows the stress dependence of LSSCW in the field of uniaxial stress.

$$\Delta V_\ell(\phi) = ½ \cdot \{[\alpha(0) + \alpha(90)] + [\alpha(0) - \alpha(90)] \cdot \cos 2\phi\}\ \sigma_y \tag{4}$$

Measurement of $\Delta V_\ell(\phi)$ in any direction ϕ allows us to determine the stress in the loading direction σ_y through eq (4). In this case, however, $\alpha(0)$ and $\alpha(90)$ should be measured in advance as material constants.

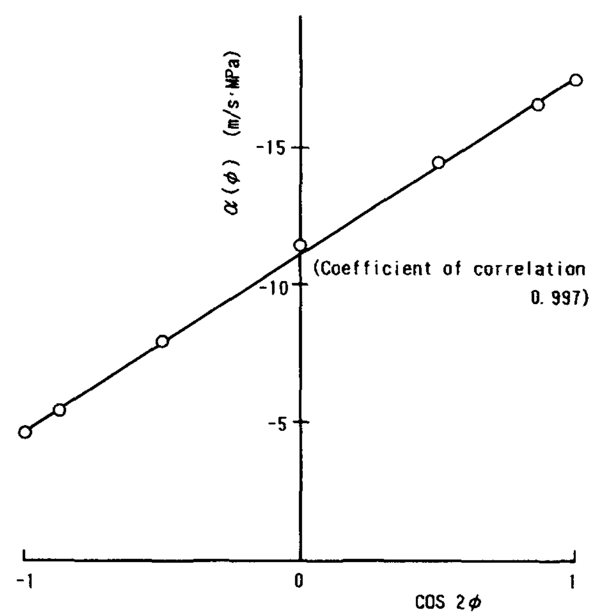

Fig. 9—Variation of slope of lines shown in Fig. 8

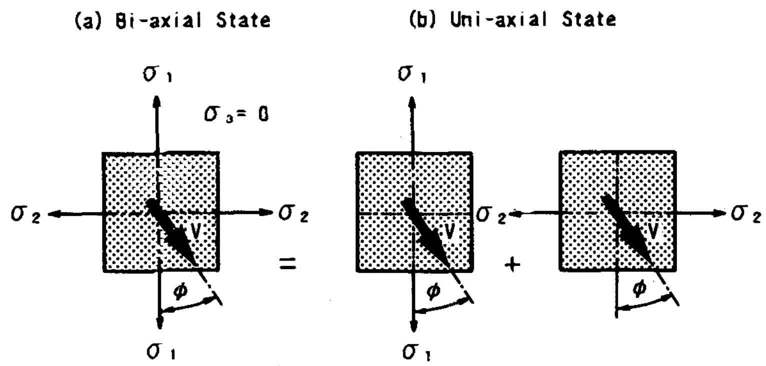

Fig. 10—Replacement of the state of biaxial stress with two states of uniaxial stress

Stress-dependence of LSSCW Velocity in the State of Biaxial Stress

Stress Dependence Developed by the Superposition Method

Consider the state of biaxial stress as shown in Fig. 10(a). In this case, two principal stresses σ_1 and σ_2 affect the velocity of propagating LSSCW. The sum of these affects upon $\Delta V_\ell(\phi)$ can be calculated by eq (4) replacing the state of biaxial stress with two states of uniaxial stress as shown in Fig. 10(b). The value of $\Delta V_\ell(\phi)$ caused by σ_1 and σ_2 can be expressed $\alpha(\phi) \cdot \sigma_1$ and $\alpha(90 - \phi) \cdot \sigma_2$ from eq (2), respectively. Therefore, $\Delta V_\ell(\phi)$ in the state of biaxial stress can be written by the sum of $\alpha(\phi) \cdot \sigma_1$ and $\alpha(90 - \phi) \cdot \sigma_2$ shown in eq (5).

$$\Delta V_\ell(\phi) = \alpha(\phi) \cdot \sigma_1 + \alpha(90 - \phi) \cdot \sigma_2 \tag{5}$$

Substituting eq (4) into eq (5), we can get eq (6) which shows the stress dependence of LSSCW in the state of biaxial stress.

$$\begin{aligned} \Delta V_\ell(\phi) &= \tfrac{1}{2} \cdot \{[\alpha(0) + \alpha(90)] \cdot (\sigma_1 + \sigma_2) \\ &\quad + [\alpha(0) - \alpha(90)] \cdot (\sigma_1 - \sigma_2) \cos 2\phi\} \qquad (6) \\ &= A \cdot (\sigma_1 + \sigma_2) + B(\sigma_1 - \sigma_2) \cos 2\phi \\ A &= [\alpha(0) + \alpha(90)]/2 \\ B &= [\alpha(0) - \alpha(90)]/2 \end{aligned}$$

Equation (6) indicates that $\Delta V_\ell(\phi)$ measurements in any three directions allow us to determine σ_1, σ_2 and ϕ. However, the validity of eq (6) should be certified by biaxial testing before applying it to actual problems because eq (6) was obtained by the superposition method.

Experimental Verification

In order to verify the validity of eq (6), biaxial tests and bending tests were made.

Biaxial Test

To generate the state of biaxial stress, the special type uniaxial specimen shown in Fig. 11 was employed. A biaxial wire strain gage was bonded to measure ϵ_1 and ϵ_2 after the specimen was machined from as-received PMMA. Dimensions of the specimen were determined by moiré and photoelasticity methods to generate the state of biaxial stress at the center part of the specimen under uniaxial loading.

In the region where the relationship between stress and strain is linear, eq (6) can be rewritten with principal

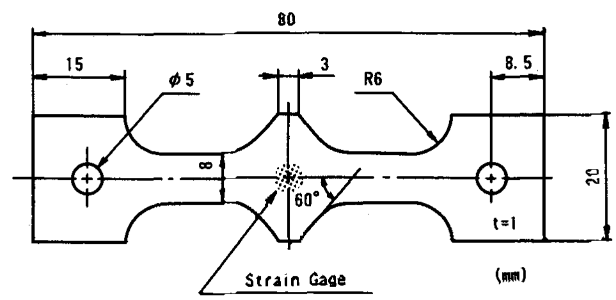

Fig. 11—Shape and dimensions of specimen for generating biaxial stress

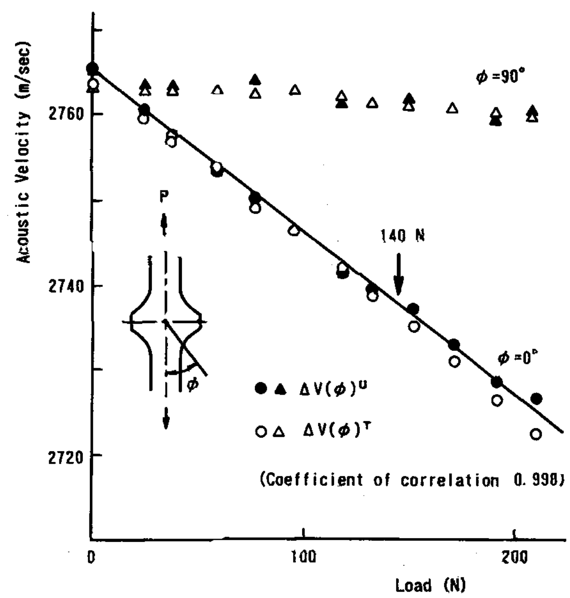

Fig. 12—Acoustic velocity (by LFB acoustic microscope) measured and calculated [by eq (7)] in the direction of ϕ = 0 deg and 90 deg

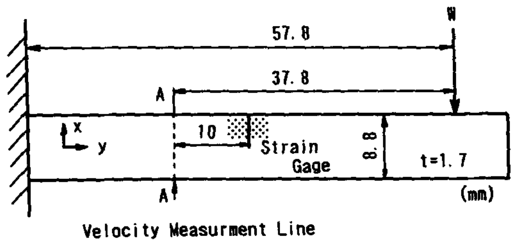

Fig. 13—Shape and dimensions of bent PMMA cantilever

strains ϵ_1 and ϵ_2 and is reduced to

$$\Delta V_\ell(\phi) = E/2 \cdot \{(\alpha(0)+\alpha(90)) \cdot (\epsilon_1+\epsilon_2)/(1-\nu) + (\alpha(0)-\alpha(90)) \cdot (\epsilon_1-\epsilon_2)\cos 2\phi/(1+\nu)\} \quad (7)$$

where E = Young's modulus and ν = Poisson's ratio, respectively. Equation (7) serves as the equation for calculating $\Delta V_\ell^T(0)$ and $\Delta V_\ell^T(90)$ from ϵ_1, ϵ_2 measured directly by the strain gages in the state of biaxial stress which were bonded at the center part of the specimen shown in Fig. 11. These values of $\Delta V_\ell^T(0)$ and $\Delta V_\ell^T(90)$ were compared with values of $\Delta V_\ell^U(0)$ and $\Delta V_\ell^U(90)$ which were measured directly by the LFB acoustic microscope in the directions of $\phi = 0$ and 90, respectively. The variations of measured and calculated values of $\Delta V_\ell(0)$ and $\Delta V_\ell(90)$ with the applied load are shown in Fig. 12. They agree well with each other in the region from P(applied load) = 0 to 140 N where stress is proportional to strain. Beyond P = 140 N, $\Delta V_\ell^T(\phi)$ is deviated from the straight line in Fig. 12 which was fitted to experimental data in the region of P = 0 N ~ 140 N by a least-squares method. However, $\Delta V_\ell^U(\phi)$s fit on the line from P = 0 N to almost fracture. From these results, eq (6) is valid.

Bending Test

The second verification was carried out through comparisons between measured and theoretical stresses σ_x and σ_y along the A-A line on a bent PMMA cantilever (Fig. 13). In a bent cantilever, σ_ys have a linear distribution. Therefore, σ_ys by the LFB acoustic microscope were plotted at the center position of LFB lens as shown in Fig. 14. Theoretical values were calculated by eq (8). In eq (8), W was determined

$$\sigma_y = WY/(bh^2/6) \quad (8)$$

where W = load, Y = distance from the loading point, and b, h = width and height of cantilever, by output from the wire strain gage (Fig. 13) comparing with a calculation curve determined in advance. It is found from Fig. 14 that eq (6) is valid in both tensile and compressional stress fields which have linear distribution.

Conclusion

The following results were obtained in this study. (1) In the case of PMMA, stress can be evaluated by the change of acoustic velocity of leaky surface skimming compressional wave (LSSCW). (2) Even if the direction

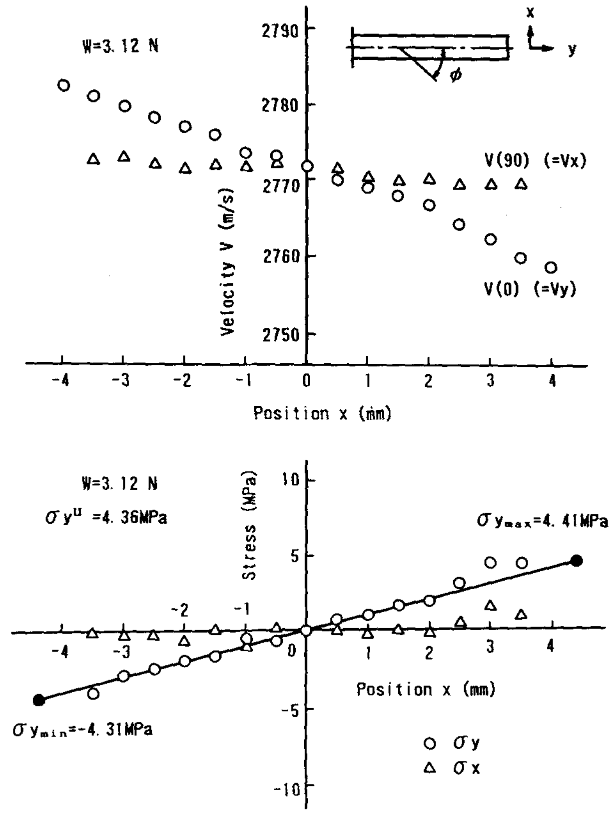

Fig. 14—Velocity and stress distribution of bent cantilever

of principal stress is unknown under the biaxial condition, the values of principal stress and its direction can be evaluated by the following procedure: (a) experimental determination of the values, V_0, $\alpha(0)$, $\alpha(90)$ in the uniaxial tensile test, (b) measurement of the acoustic velocities in the three different directions of ϕ, (c) calculation of σ_1, σ_2 and ϕ by using eq (3) and eq (5).

Acknowledgment

This study has been conducted with the financial support from the 14th Mitsubishi Science Foundation and Japan Academic Science Promotion, grant No. 61104001. We also thank Professor N. Chubachi for his helpful suggestions with the operation of SAM.

References

1. Pasley, R.L., "Barkhausen Noise Effect," *Mat. Eval.*, **28**, 157-161 (1970).
2. Furuya, Y. and Shimada, H., "Evaluation of Material Strength by Magnetic Barkhausen Noise Analysis," *Japan NDI*, **35** (8), 532-537 (1986).
3. Fukuoka, H., "Stress Analysis by Acoust Elasticity," *Trans. JSME(A)***49** (440), 403-412 (1983).
4. Remons, R.A. and Quate, C.F., "A Scanning Acoustic Microscope," *Proc. IEEE Ultrasonic Symposium*, 18-21 (1973).
5. Kushibiki, J. and Chubachi, N., "Material Characterization by Line-Focus-Beam Acoustic Microscope," *IEEE Trans. Sonics. Ultrason.*, SU-32, 189-212 (1985).
6. Hayes, M. and Rivlin, R.S., "Surface Wave in Deformed Elastic Materials," *Arch. Rat. Mech. Anal.*, **8**, 358 (1961).
7. Jassby, K. and Kisoni, D., "Experimental Technique for Measurement of Stress-acoustic Coefficient of Rayleigh Wave," EXPERIMENTAL MECHANICS, **23**, 74-80 (1983).